

# Passively mode-locked 10 GHz femtosecond Ti:sapphire laser

A. Bartels,<sup>1,2,\*</sup> D. Heinecke,<sup>2</sup> and S. A. Diddams<sup>3</sup>

<sup>1</sup>Gigaoptics GmbH, Blarerstrasse 56, 78462 Konstanz, Germany

<sup>2</sup>Center for Applied Photonics, University of Konstanz, Universitätsstrasse 10, 78457 Konstanz, Germany

<sup>3</sup>National Institute of Standards and Technology, 325 Broadway M.S. 847, Boulder, Colorado 80305, USA

\*Corresponding author: bartels@gigaoptics.com

We report a mode-locked Ti:sapphire femtosecond laser emitting 42 fs pulses at a 10 GHz repetition rate. When operated with a spectrally integrated average power greater than 1 W, the associated femtosecond laser frequency comb contains  $\sim 500$  modes, each with power exceeding 1 mW. Spectral broadening in nonlinear microstructured fiber yields comb elements with individual powers greater than 1 nW over  $\sim 250$  nm of spectral bandwidth. The modes of the emitted comb are resolved and imaged with a simple grating spectrometer and digital camera. Combined with absorption spectroscopy of rubidium vapor, this approach permits identification of the mode index and measurement of the carrier envelope offset frequency of the comb.

OCIS codes: 140.7090, 120.3940, 320.7160.

Many scientific and technological applications of femtosecond lasers benefit from sources with repetition rates of several gigahertz that have become available in the recent past [1–5]. Novel real-time ultrafast optical sampling techniques benefit from sub-100 fs pulses at repetition rates of several gigahertz because they permit a better time resolution [6]. In the frequency domain, the high power per mode in a multigigahertz femtosecond laser frequency comb (FLFC) is a benefit to direct frequency comb spectroscopy [7], length metrology [8], and applications such as the development of optical clocks [9] and low-noise microwave generation [10,11]. Emerging applications such as the frequency comb calibration of high-resolution astronomical spectrographs [12–14] and the synthesis of optical and microwave waveforms via line-by-line pulse shaping [15] both require large optical bandwidths and a frequency comb with a repetition rate sufficiently high that the modes are easily resolved with a spectrometer.

There are numerous semiconductor, fiber-based, and solid-state mode-locked sources that operate at a repetition rate of 10 GHz (or higher), but these all produce low-power pulses having durations in the 1–10 ps range [16–19]. Sub-100 femtosecond durations at 10 GHz have been achieved at 1550 nm but only with extracavity soliton compression techniques in dispersion-decreasing fiber [3]. Moreover, many high-repetition-rate lasers rely on active harmonic mode locking, which can suffer from frequency and timing jitter noise intrinsic to microwave sources or the supermodes. These problems are largely avoided in fundamentally mode-locked systems that passively employ the Kerr nonlinearity.

In this Letter, we demonstrate a 10 GHz passively mode-locked Ti:sapphire laser that directly outputs a unique combination of large fractional bandwidth, high repetition rate, and high average power. The resulting pulses are as short as 42 fs and still higher repetition rates appear possible. The high repetition rate allows the individual modes of the emitted FLFC

to be resolved with a simple grating spectrometer. This would enable the frequency comb to be interfaced with existing spatial light modulators for line-by-line pulse shaping. Additionally, high-resolution spectroscopy techniques directly utilizing the frequency comb should benefit from the high repetition rates and the enhancement of available power per mode [7]. Along these lines, we use direct comb spectroscopy of rubidium vapor at 780 nm to effectively measure the carrier-envelope offset frequency, when the repetition rate is locked to a microwave reference. Finally, we show that even with relatively low-energy pulses ( $\sim 60$  pJ), the femtosecond duration provides peak powers sufficient for modest spectral broadening in nonlinear microstructured fiber. When referenced to stable optical and/or microwave frequency standards, the broadened comb would be valuable for numerous applications, including recent efforts aimed at calibrating high-resolution astronomical spectrographs [12–14].

The ring cavity design follows that of earlier work [see Fig. 1(a)] [5]; however, specially designed mechanics and optics were required to achieve the high repetition rate and corresponding small size. A Ti:sapphire crystal 1.5 mm long is pumped through mirror M1 with a lens of 30 mm focal length by 6.5 W from a 532 nm laser. Both adjacent focusing mirrors M1 and M2 have a radius of curvature of 8 mm. Mirror M3 and the output coupler OC complete the X-folded ring cavity. The total cavity length is 3 cm, yielding a repetition rate of 10 GHz. Mirrors M1–M3 have a highly reflective negative dispersive coating with approximately  $-40$  fs<sup>2</sup> group-delay dispersion (GDD) between 750 and 850 nm. Together with the laser crystal the net cavity GDD is approximately  $-35$  fs<sup>2</sup>. Output couplers with 1% and 2% transmission are used. Mirror M2 is brought close to the inner edge of the cavity stability range where pulsed operation is usually self-starting. When mode locked, the laser operates unidirectionally in a random direction. We restart mode locking until operation in the direc-

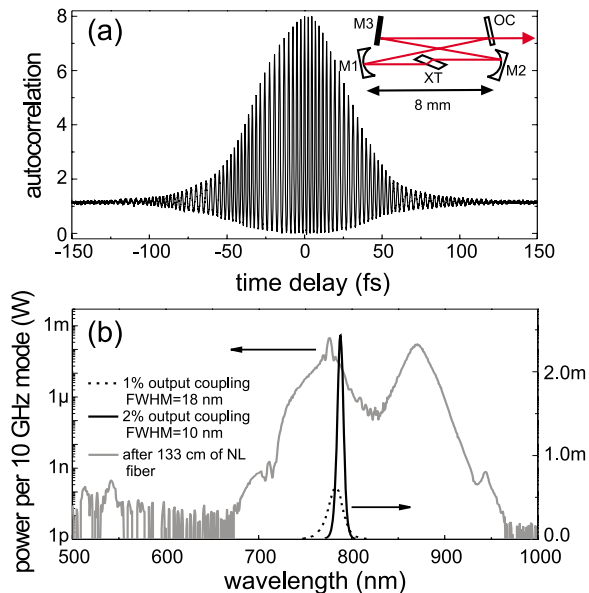


Fig. 1. (Color online) (a) Interferometric autocorrelation trace of 42 fs pulses with 1% output coupler. Inset, schematic of laser cavity; XT is the Ti:sapphire crystal. (b) The black curves show laser output spectra at 1% and 2% output coupling on a linear scale. The gray curve shows the spectrum after broadening in nonlinear fiber on a logarithmic scale.

tion indicated in Fig. 1 is obtained. The laser yields 650 mW of mode-locked output power with the 1% output coupler and 1.06 W with the 2% output coupler. Interferometric autocorrelation traces and intensity spectra were acquired for both output couplers. At 1% output coupling, 42 fs pulses are emitted, assuming a  $\text{sech}^2$  pulse envelope [see Fig. 1(a)]. The spectral FWHM is 18 nm centered around 783 nm wavelength [see Fig. 1(b)]. The power per mode is more than  $300 \mu\text{W}$  within the FWHM. At 2% output coupling 69 fs pulses are obtained with a corresponding spectral bandwidth of 10 nm centered at 788 nm. In this case, the power per mode is as large as 2.4 mW at the spectral peak. Thus, there are more than 500 modes with a precise 10 GHz spacing and  $>1$  mW of power per mode. With both values of output coupling the pulses are close to the transform limit.

Additional spectral broadening is achieved in nonlinear microstructured fiber that has a  $1.5 \mu\text{m}$  core and zero dispersion wavelength near 590 nm, which was a good match for low-power Ti:sapphire sources [20]. With the 1% output coupling, approximately 220 mW is coupled into the microstructured fiber, corresponding to a pulse energy and peak power of 22 pJ and 550 W, respectively. While this is insufficient for the generation of an octave-spanning spectrum that would enable self-referencing, significant broadening of the spectrum still occurs [Fig. 1(b)], and powers at or greater than 1 nW per mode exist over nearly 250 nm. Such power levels are sufficient for use in heterodyne measurements with cw lasers as well for the calibration of astronomical spectrographs [12]. A small amount of green light near 540 nm is also visible in the spectrum of Fig. 1(b).

The output pulse train is detected by focusing  $\sim 10$  mW of optical power onto a 25 GHz bandwidth photodetector; Fig. 2 shows the resulting microwave spectrum of the photocurrent. A clean spectrum shows only the 10 GHz repetition rate and the second harmonic above the noise floor of the spectrum analyzer. No evidence of Q switching is observed. With a GaAs photodetector an electrical power as high as  $-6$  dBm at 10 GHz is obtained for an average current of  $\sim 4$  mA. Such high power levels obtained via photo-detection of mode-locked optical pulse trains are of value for the generation of low-noise microwave signals relative to optical references [10,11].

The individual FLFC elements are resolved with a spectrometer consisting of a 2400 lines/mm grating and a lens with a 77 cm focal length that images the modes onto a CCD. The laser beam diameter is first expanded to 1.5 cm and the angle of incidence on the grating is approximately  $63^\circ$ . Figures 3(a)–3(d) are four false-color images of a few of the resolved modes near the rubidium  $D_2$  line at 780 nm. The power in each mode that passes through a pinhole of  $100 \mu\text{m}$  diameter is  $170 \mu\text{W}$ , corresponding to an efficiency greater than 34% for the spectrometer. With optimized grating and optics, one could anticipate resolving the individual modes with an efficiency greater than 90%.

The repetition rate of the laser was locked to a stable microwave reference at 10.2288973 GHz and incremented over 234 kHz in the steps given in Figs. 3(a)–3(d). Figure 3(e) shows line scans through three of the CCD images, illustrating the measured  $\sim 6$  GHz resolution of the spectrometer, which is limited by the choice of lens and number of grating lines illuminated. In Figs. 3(b) and 3(d) the repetition rate of the laser is adjusted such that one mode is absorbed by an isotopically pure vapor of  $^{87}\text{Rb}$  contained in a cell 5 cm long that is heated to  $55^\circ\text{C}$ . The two absorption features arise from transitions between the two resolved hyperfine levels (separated by  $\sim 6.8$  GHz) of the  $5^2S_{1/2}$  ground state and the unresolved hyperfine levels of the  $5^2P_{3/2}$  excited state [21]. By tuning the comb mode between the two absorption peaks, we determine this mode index to be 37,563

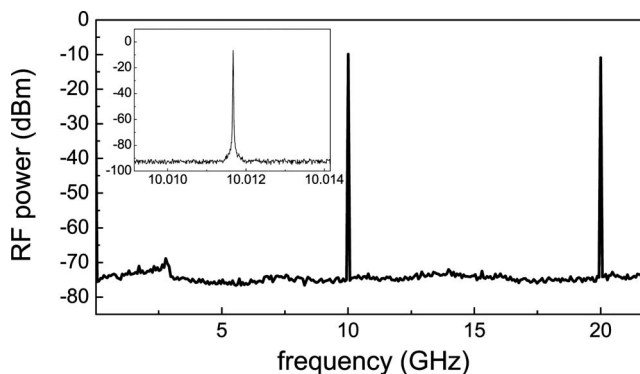


Fig. 2. RF spectrum of photocurrent obtained by detecting the pulse train with a 25 GHz photoreceiver. The resolution bandwidth (RBW) was 100 kHz. Inset, repetition rate signal acquired with a 5 MHz span and 3 kHz RBW. In both spectra the noise floor is that of the spectrum analyzer.

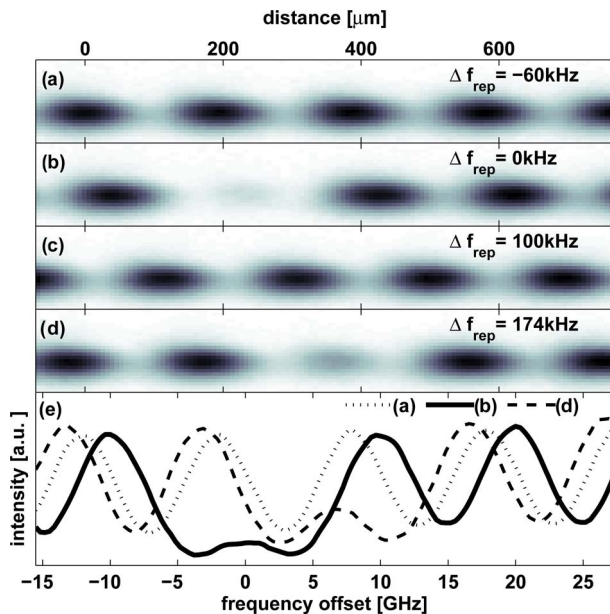


Fig. 3. (Color online) (a)–(d) Resolved frequency comb modes near the Rb  $D_2$  line recorded with a CCD camera at different offsets of the repetition rate from 10.2288973 GHz. The top axis indicates the position on the CCD array, which has a pixel spacing of  $6.7 \mu\text{m}$ . The two absorption features in (b) and (d) arise from transitions between the two resolved hyperfine levels of the  $5^2S_{1/2}$  ground state and the unresolved hyperfine levels of the  $5^2P_{3/2}$  excited state. (e) Line scans through images (a), (b), and (d).

and the carrier envelope offset frequency is  $\sim 0.14$  GHz. In this straightforward spectroscopy, the uncertainty in tuning the mode to the maximum absorption is estimated to be  $\sim 50$  MHz, or roughly  $1/10$  of the Doppler-broadened width. Based on the known optical frequency of the  $D_2$  transition and the locked value of the repetition rate, the frequencies of all of the modes of the comb can be determined with the same uncertainty. This spatially resolved comb is an array of  $\sim 1000$  cw modes with atomically referenced frequencies and powers at the  $100 \mu\text{W}$  level. The presently achieved frequency precision of  $1 \times 10^{-7}$  could already be useful for some applications. However, the power in an individual mode is sufficient to perform saturated absorption spectroscopy of the same rubidium transitions, which could provide an improvement in precision of 3 orders of magnitude [21].

In conclusion, the 10 GHz repetition rate reported here is a significant advance in the Ti:sapphire wavelength regime, because a simple grating-based spectrometer is sufficient to separate the individual modes for applications in waveform generation, direct frequency comb spectroscopy, and the calibration of astronomical spectrographs. The Ti:sapphire wavelength and 10 GHz mode spacing have good overlap with useful atomic systems (e.g., Rb and Cs), which can provide an atomically referenced and spectrally resolved FLFC with precision at the  $10^{-10}$  level. Higher repetition rates appear possible because the nonlinear phase-shift in the cavity is still about a fac-

tor of 2 above that of similar systems demonstrated earlier [2].

We thank Svenja Knappe for providing the rubidium vapor cell along with Leo Hollberg and Danielle Braje for helpful advice and discussions. We further thank Long-Sheng Ma and Shijun Xiao for thoughtful comments on this manuscript. Funding for this work was provided in part by the National Institutes of Standards and Technology (NIST) and the Defense Advanced Research Projects Agency (DARPA).

## References

1. B. C. Collings, K. Bergman, and W. H. Knox, *Opt. Lett.* **14**, 1098 (1997).
2. A. Bartels, T. Dekorsy, and H. Kurz, *Opt. Lett.* **24**, 996 (1999).
3. K. R. Tamura and M. Nakazawa, *Opt. Lett.* **26**, 762 (2001).
4. C. G. Leburn, A. A. Lagatsky, C. T. A. Brown, and W. Sibbett, *Electron. Lett.* **40**, 805 (2004).
5. A. Bartels, R. Gebs, M. S. Kirchner, and S. A. Diddams, *Opt. Lett.* **32**, 2553 (2007).
6. A. Bartels, R. Cerna, C. Kistner, A. Thoma, F. Hudert, C. Janke, and T. Dekorsy, *Rev. Sci. Instrum.* **78**, 035107 (2007).
7. M. C. Stowe, M. J. Thorpe, A. Pe'er, J. Ye, J. E. Stalnaker, V. Gerginov, and S. A. Diddams, in *Advances in Atomic, Molecular and Optical Physics*, E. Arimondo and P. Berman, eds. (Elsevier, 2007), Vol. 55.
8. J. Jin, Y.-J. Kim, Y. Kim, S.-W. Kim, and C.-S. Kang, *Opt. Express* **14**, 5968 (2006).
9. S. A. Diddams, Th. Udem, J. C. Bergquist, E. A. Curtis, R. E. Drullinger, L. Hollberg, W. M. Itano, W. D. Lee, C. W. Oates, K. R. Vogel, and D. J. Wineland, *Science* **293**, 825 (2001).
10. A. Bartels, S. A. Diddams, C. W. Oates, G. Wilpers, J. C. Bergquist, W. H. Oskay, and L. Hollberg, *Opt. Lett.* **30**, 667 (2005).
11. J. J. McFerran, E. N. Ivanov, A. Bartels, G. Wilpers, C. W. Oates, S. A. Diddams, and L. Hollberg, *Electron. Lett.* **41**, 36 (2006).
12. M. Murphy, T. Udem, R. Holzwarth, A. Sizmann, L. Pasquini, C. Araujo-Hauck, H. Dekker, S. D'Odorico, M. Fischer, T. W. Hänsch, and A. Manescau, *Mon. Not. R. Astron. Soc.* **380**, 839 (2007).
13. D. A. Braje, M. S. Kirchner, S. Osterman, T. M. Fortier, and S. A. Diddams, *Eur. Phys. J. D* **48**, 57 (2008).
14. C.-H. Li, A. J. Benedick, P. Fendel, A. G. Glenday, F. X. Kärtner, D. F. Phillips, D. Sasselov, A. Szentgyorgyi, and R. L. Walsworth, *Nature* **452**, 610 (2008).
15. Z. Jiang, D. E. Leaird, and A. M. Weiner, *Opt. Express* **13**, 10431 (2005).
16. F. Quinlan, S. Gee, S. Ozharar, and P. J. Delfyett, *Opt. Lett.* **31**, 2870 (2006).
17. E. Yoshida and M. Nakazawa, *Electron. Lett.* **34**, 1753 (1998).
18. R. Paschotta, L. Krainer, S. Lecomte, G. J. Spühler, S. C. Zeller, A. Aschwanden, D. Lorenser, H. J. Unold, K. J. Weingarten, and U. Keller, *New J. Phys.* **6**, 174 (2004).
19. S. C. Zeller, T. Südmeyer, K. J. Weingarten, and U. Keller, *Electron. Lett.* **43**, 32 (2007).
20. M. Kirchner, T. Fortier, A. Bartels, and S. A. Diddams, *Opt. Lett.* **14**, 9531 (2006).
21. J. Ye, S. Swartz, P. Jungner, and J. L. Hall, *Opt. Lett.* **21**, 1280 (1996).